INTERNATIONAL JOURNAL OF PRECISION ENGINEERING AND MANUFACTURING Vol. 18, No. 6, pp. 879-885 JUNE 2017 / 879

REGULAR PAPER

DOI: 10.1007/s12541-017-0104-6
ISSN 2234-7593 (Print) / 2005-4602 (Online)

Optimal Seat and Footrest Positions of Manual Standing Wheelchair

Jeseong Ryu[1], Jongsang Son[2,3], Min Jo[1], Eunkyoung Choi[1], Soonjae Ahn[1], Sinki Kim[4], and Young-ho Kim[1,#]

1 Department of Biomedical Engineering, Yonsei University, 1, Yeonsedae-gil, Heungeop-myeon, Wonju-si, Gangwon-do, 26493, South Korea
2 Sensory Motor Performance Program, Rehabilitation Institute of Chicago, Chicago, IL 60611, USA
3 Department of Physical Medicine & Rehabilitation, Northwestern University, Chicago, IL 60611, USA
4 Korea Orthopedics & Rehabilitation Engineering Center, 26, Gyeongin-ro 10 beon-gil, Bupyeong-gu, Incheon, 21417, South Korea
Corresponding Author / E-mail: younghokim@yonsei.ac.kr, TEL: +82-33-760-2492, FAX: +82-33-760-2806

KEYWORDS: Optimal hand rim position, Wheelchair dynamometer, Planar link-segment model, Propulsion energy

A standing wheelchair is highly recommended to an individual suffering from secondary complications due to long-term sitting in a standard wheelchair. However, the newly-designed standing wheelchair has hand rims separate from the wheels, likely affecting the biomechanical characteristics and the efficiency of propulsion. The objectives of this dissertation were aimed to propose a method to determine the optimal riding position by evaluating energy expenditure during manual standing wheelchair propulsion. Ten elderly male subjects were asked to propel the hand rims with nine different seat (while sitting) and footrest (while standing) positions. During the experiments, kinematic and kinetic data were simultaneously obtained using a 3D motion capture system and a brake-type wheelchair dynamometer, respectively. Upper-limb joint torques and total propulsion energy were determined using a planar link-segment model with the optimization technique based on minimal joint torque criteria. Shorter subjects had the lowest total propulsion energy expenditure in the downward-forward and middle-forward positions, while closest to the hand rims. However, taller subjects had the lowest total propulsion energy expenditure in the downward-center and middle-center positions, while a little further from the hand rims. We believe that these methods and results will be helpful in assessing the adequacy of the riding position of various types of wheelchair.

Manuscript received: November 20, 2016 / Revised: February 16, 2017 / Accepted: February 19, 2017

1. Introduction

Wheelchair is one of the important transportations for individuals with loss of mobility; however, its long-term use is associated with various upper extremity injuries.[1] Subbarao and colleagues[2] reported that approximately 73% of manual wheelchair users with spinal cord injury (SCI) experience chronic shoulder and/or wrist pain. Since these upper extremity injuries are highly responsible for both independence and quality of life of an individual, previous studies have been conducted to determine what factor would be associated with such pain and injury.

Considering that an overuse of the arm in an inefficient manner may be related to such pain and injury, many studies have evaluated the effects of seat position or propulsion pattern on physiological and biomechanical outcomes. Brubaker[3] showed that a posterior seat position has a lower rolling resistance and requires less energy to propel. Van der Woude et al.[4] reported that various cardiorespiratory responses (e.g., oxygen cost, ventilation, and heart rate) increased with increasing seat height and suggested the optimum seat height as the height at where the elbow flexion angle ranges from 60-80° when the user grips the top dead center (TDC) of the hand rim. According to a previous study[5] regarding changes in the propulsion pattern and muscle activity depending on six different seat positions, the backward-low position had the overall lowest integrated electromyography (IEMG) with smoother motions of the elbow and forearm. In addition, Kotajarvi et al.[6] examined the effects of seat position on the efficiency of push force during manual wheelchair propulsion and concluded that the tangential force output did not significantly change with seat position and that the axial and radial forces were largest in the lowest and posterior seat position. These imply that the relative position of the hand rim with respect to a wheelchair user affects the propulsion efficiency that may be associated with the upper extremity pain and injury.

Since long-term sitting in a wheelchair often causes painful, problematic, and costly secondary complications, a standing wheelchair is highly recommended with many benefits, such as improvements in health-related problems (e.g., better circulation, reduction of abnormal

muscle tone and spasticity, and lower occurrence of pressure sores).[7] Moreover, standing allows much larger working areas, thereby providing better functional activities of daily living, independence, and productivity. However, hand rims are typically separated from the wheels for providing both sitting and standing postures in a standing wheelchair; thus, it may affect the relative hand rim positions and in turn the propulsion efficiency. Considering that most wheelchair users are elderly as a result of sudden onset of disability (e.g., SCI, stroke), gradual onset of progressive disease (e.g., osteoarthritis, multiple sclerosis), or loss of walking mobility,[8,9] investigations regarding the effects of the relative position of the hand rim with respect to the user on the propulsion efficiency should be conducted to suggest an optimal design of a standing wheelchair.

In this study, the total mechanical energy of the upper-limb joints at nine different positions was evaluated to determine an optimal position of the hand rims with respect to the user during manual propulsion and sitting/standing in a standing wheelchair. During the manual propulsion, the upper-limb kinematics and the propulsion torque were measured, thereby predicting the joint moments and total propulsion energy expenditure using a planar link-segment model with an optimization technique.[10-14] The hypothesis of this study was that the optimal position would be different depending on the height of the user and the posture (i.e., sitting and standing) as well.

2. Methods

2.1 Apparatus of the brake-type wheelchair dynamometer and manual standing wheelchair

Our brake-type dynamometer has been developed to measure the torques and RPMs during the propulsion of various wheelchairs.[12-14] It consists of two dynamometers for each wheel and two support frames for the front and rear casters. Each dynamometer has a roller (Φ200× 400 mm, steel tubular), torque sensor (TMA-2KM, Setech Co., Ltd., KR) with an RPM sensor (MP-981, Setech Co., Ltd., KR), and powder brake (PRB-1.2Y3, Pora electric machinery Co., Ltd., KR) connected in series, using shafts and bearings. Thus, it can measure both roller-axis torque and RPMs generated by a wheel during the propulsion. Finally, these can be used to determine the wheel-axis torque, RPM, and propulsion tangential force.

The powder brake can control the roller-axis rolling resistance by the voltage control knob. The minimum rolling resistance is 0 N·m at 0 V, and the maximum is 17 N·m at 24 V. In this study, the rolling resistance was set at 0.55 N·m (at 3 V) because such setting best simulated the laboratory floor (carpet) condition.

A prototype of the manual standing wheelchair (HANIL Hightech Co., Ltd., KR) was installed on the dynamometer system (Fig. 1). The manual standing wheelchair has two hand rims separated from each wheel enabling their use in the standing position as well. The diameters of the hand rim and wheel were 320 and 380 mm, respectively. The seat was 380 mm wide and 400 mm deep. The seat's backrest was 35.3 cm behind and 3.2 cm below the hand rim center. The footrest was 92 cm below the hand rim center. The initial positions of the seat and footrest were defined as the original positions (middle-center). The dimensions of the standing wheelchair were determined by the manufacturer according to the anthropometric data of normal adults.

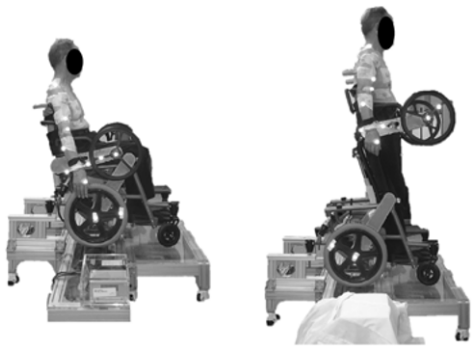

Fig. 1 Experimental setup for the standing wheelchair prototype installed on our brake-type dynamometer

Table 1 Subject characteristics (mean ± SD)

Characteristics	Short group N = 5	Tall group N = 5	*p*-value*
Age (y)	76.4 ± 1.9	75.4 ± 2.9	0.538
Mass (kg)	55.9 ± 10.2	66.0 ± 9.1	0.138
Height (cm)	160.2 ± 2.9	166.6 ± 1.6	0.003

* Unpaired *t*-test, significant difference between groups ($p < 0.05$)

2.2 Experiment procedure

Ten elderly male subjects participated in this study (Table 1). Prior to the experiment, all participants provided an informed written consent, which were approved by the Institutional Review Board of Yonsei University (No. 1041849-201406-BM-029-01). Seven spherical reflective markers (14 mm in diameter) were attached to the subjects' right upper limb according to the Plug-In-Gait model (Oxford Metrics Ltd., UK). Two additional markers were positioned at the rotation center of the hand rim and the middle of the hand rim spoke to directly measure the RPMs of the hand rim. The subjects were asked to sit on the standing wheelchair, leaning back on the backrest and to familiarize themselves with the propulsion of the standing wheelchair for 2-3 minutes. Thereafter, they were also requested to propel the hand rims with different seat and footrest positions at their self-selected speed.

To determine the relative position of the hand rim, nine different positions were chosen as follows: original position (middle-center, MC); 6 cm forward from the MC (middle-forward, MF); 6 cm backward from the MC (middle-backward, MB); 6 cm upward from the MC (up-center, UC); 6 cm forward from the UC (up-forward, UF); 6 cm backward from the UC (up-backward, UB); 6 cm downward from the MC (down-center, DC); 6 cm forward from the DC (down-forward, DF); and 6 cm backward from the DC (down-backward, DB) as shown in Fig. 2. The sitting posture was tested first, followed by the standing posture. The subjects propelled six times at each position assigned randomly.

During the experiments, the marker trajectories were recorded at 200 Hz, using a 3D motion capture system (Vicon MX system, Vicon Motion System Ltd., UK). In addition, the analog data measured from the dynamometer were simultaneously obtained at 1 kHz, using an

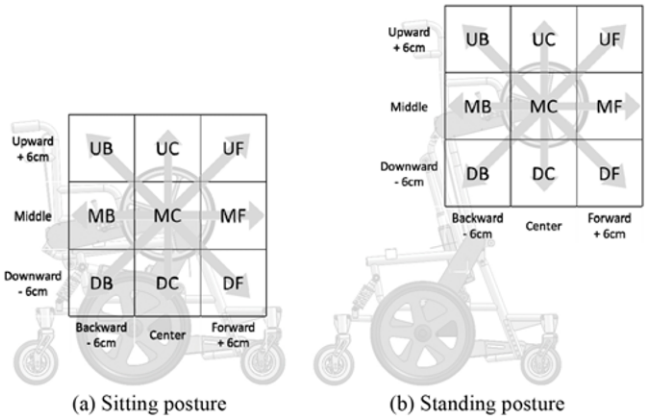

Fig. 2 Distance between the hand and hand rim: Nine positions in the sitting and standing posture

analog sync box (Vicon MX system, Vicon Motion System Ltd., UK).

2.3 Optimization methods and data analysis

Upper-limb joint moments and total propulsion energy were determined using a planar link-segment model with an optimization technique (Fig. 3).[10-14] To calculate the shoulder, elbow, and wrist joint moments, the propulsion force ($\overrightarrow{F_p}$), which is the unknown variable, should be calculated first. The propulsion force ($\overrightarrow{F_p}$) consists of the tangential force ($\overrightarrow{F_t}$) and the radial force ($\overrightarrow{F_r}$), and the tangential force can be calculated from the roller torque ($\overrightarrow{T_r}$) which is measured using the dynamometer system. Thus, the unknown variable $\overrightarrow{F_r}$, the radial force, can be determined by formulating an optimization problem minimizing the summation of the difference between the measured and calculated wheel-axis torques and each joint moment (Eq. (1)).

$$\text{Min}\left\{\left(T_r-\frac{\left|\overrightarrow{r_r}\right|}{\left|\overrightarrow{OH}\right|}T_h\right)^2+T_S^2+T_E^2+T_W^2\right\} \tag{1}$$

where

$$T_h=\left|\overrightarrow{OH}\times\overrightarrow{F_p}\right|$$

$$\overrightarrow{F_p}=\overrightarrow{F_t}+\overrightarrow{F_r}$$

$$T_w=\frac{\overrightarrow{r_w}}{\overrightarrow{OH}}T_h$$

$$T_r=\frac{\overrightarrow{r_r}}{\overrightarrow{r_w}}T_w$$

$$T_S=\left|\overrightarrow{SH}\times\overrightarrow{F_p}\right|$$

$$T_E=\left|\overrightarrow{EH}\times\overrightarrow{F_p}\right|$$

$$T_W=\left|\overrightarrow{WH}\times\overrightarrow{F_p}\right|$$

where T_S, T_E, and T_W indicate the shoulder, elbow, and wrist joint moments, respectively; $\overrightarrow{SH}$, $\overrightarrow{EH}$, $\overrightarrow{WH}$, and $\overrightarrow{OH}$ represent the position vectors from each shoulder, elbow, and wrist joint center to the point of force application on the hand rim and the wheel-axis to the point; T_h, T_w, and T_r are the hand rim, wheel, and roller torques, respectively.

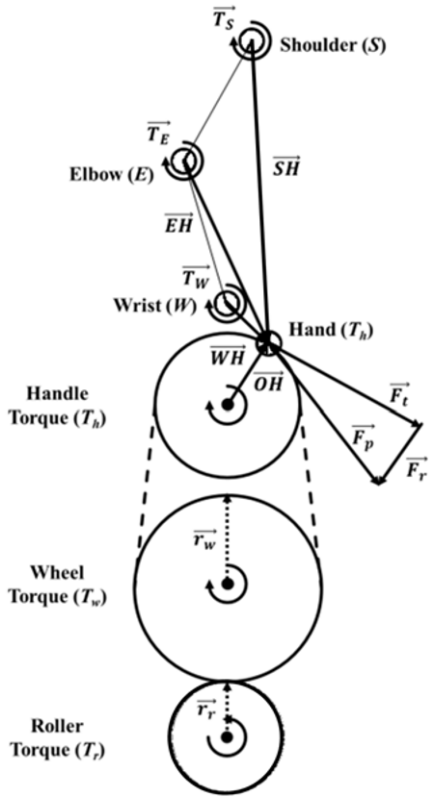

Fig. 3 Schematic diagram of the planar link-segment model (see Eq. (1) for a detailed explanation of the variables)

Two-dimensional kinematics for the shoulder, elbow, and wrist joints were calculated using reflective markers in the sagittal plane. As the subjects were leaning back on the backrest of the standing wheelchair fixed on the dynamometer system, the shoulder joint angle was defined as the angle between the backrest and the upper arm segment. Similarly, the elbow and wrist joint angles were the angles between the upper arm and the forearm segments and between the forearm and the hand segments, respectively. For all the joints, a positive angle represents flexion. Propulsion angles were also determined as the wheel rotation angle during the contact phase. The total mechanical energy expenditure is the sum of the shoulder, elbow, and wrist joint energy expenditures. Each joint energy expenditure was divided by the sum of the positive joint power to the maximum wheel RPM. Each joint power was calculated by multiplying the joint moment and the angular velocity of each joint.

2.4 Statistical analysis

All statistical analyses were performed using the IBM SPSS Statistics (Version 22, IBM Corp., USA). Repeated measures analysis of variance was applied with the position of the hand rim as the main factor to detect significant differences in the biomechanical variables. An unpaired *t*-test was performed to compare the subject groups' characteristics. Based on a significant level of $p < 0.05$, post hoc analyses were conducted and corrected for multiple comparisons using LSD tests.

Table 2 Optimal seat position for the different groups and conditions

Group		Vertical position	Horizontal position
Sitting	Short	Middle	Forward
	Tall	Upward	Backward
Standing	Short	Middle	Center
	Tall	Upward	Center

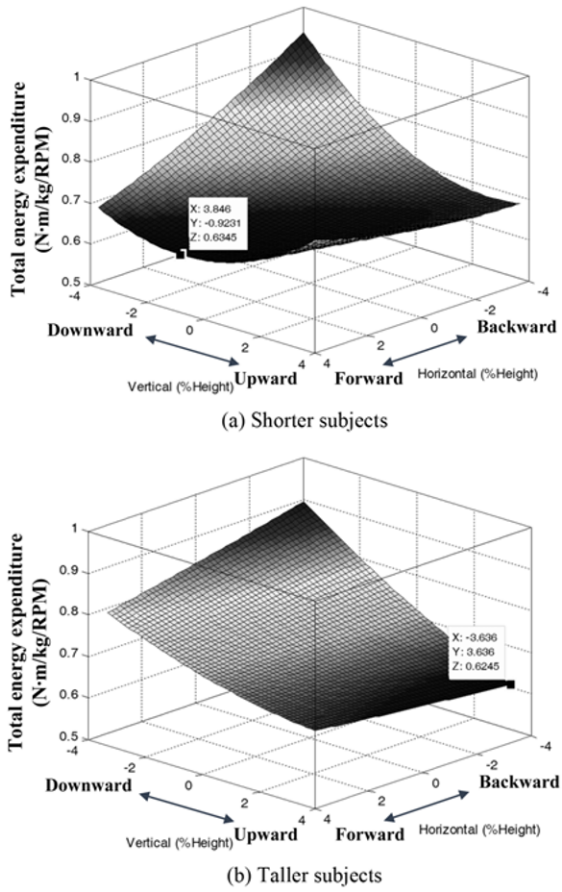

Fig. 4 Surface fitting of the optimal position for the sitting posture

3. Results

3.1 Total propulsion energy

We assumed that the optimal position would have the lowest total energy expenditure. For the propulsion energy in the sitting posture, the subjects with a shorter stature had the lowest total propulsion energy in the MF position, while the taller subjects had the lowest total propulsion energy in the UB position (Table 2). For the propulsion energy in the standing posture, the shorter subjects had the lowest total propulsion energy in the MC position, while the taller subjects had the lowest total propulsion energy in the UC position (Table 2).

3.2 Optimal seat position during sitting

Fig. 4 shows the optimal sitting position for the elderly subjects. The lowest total energy expenditure was shown at the position of (0.9% downward, 3.8% forward) for the shorter subjects and (3.6% upward, 3.6% backward) for the taller subjects compared to the original position.

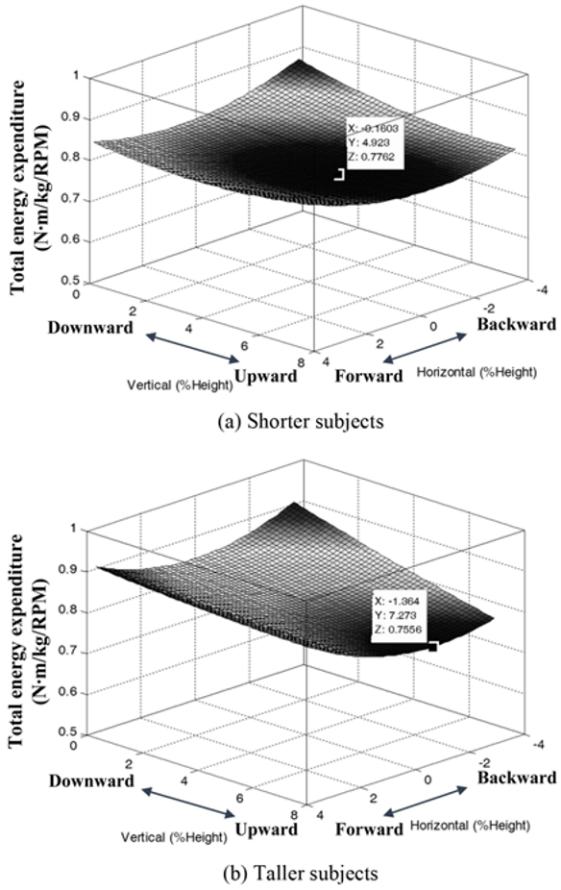

Fig. 5 Surface fitting of the optimal position for the standing posture

3.3 Optimal footrest position during standing

Fig. 5 shows the optimal standing position for the elderly subjects. The lowest total energy expenditure was shown at the position of (0.9% upward, 0.2% backward) for the shorter subjects and (3.3% upward, 1.4% backward) for the taller subjects compared to the original position.

3.4 Energy expenditure ratio (EER) per propulsion angle

Fig. 6 shows the propulsion angle in each position for both groups in the sagittal plane. In the sitting posture, the propulsion angle was the smallest in the UB position and became gradually larger until the DF direction was reached (Fig. 6(a)). For the shorter subject group, the smallest propulsion angle was 109.6° ± 17.7 in the UB position, and the largest propulsion angle was 166.9° ± 39.2 in the DF position. Five positions (MC, MF, DB, DC, and DF) had mean propulsion angles over 140°. The downward positions had significantly larger propulsion angles than the upward positions ($p < 0.05$). For the taller subject group, the smallest propulsion angle was 109.9° ± 21.4 in the UB position, and the largest propulsion angle was 148.4° ± 34.7 in the MF position. Only three positions (MF, DC, and DF) had mean propulsion angles over 140°. For the shorter subject group in the standing posture, the smallest propulsion angle was 131.1° ± 29.1 in the UB position, and the largest propulsion angle was 159.0° ± 37.7 in the DF position (Fig. 6(b)). Seven positions had mean propulsion angles over 140°, except for the UB and UC positions. For the taller subject group, the smallest propulsion angle was 130.5° ± 29.6 in the UB position, and the largest

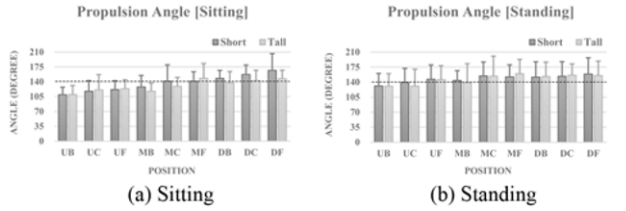

Fig. 6 Mean values of the propulsion angle at each position

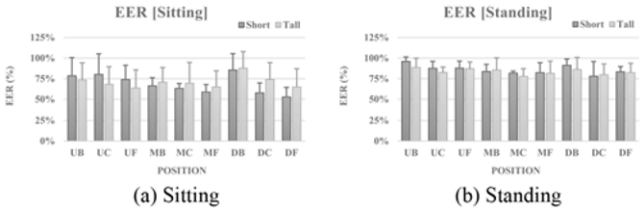

Fig. 7 Mean values of the energy expenditure ratio per propulsion angle at each position

propulsion angle was 159.5° ± 33.5 in the MF position. Six positions had mean propulsion angles over 140°, except for the UB, UC, and MB positions. However, significant differences were not found according to each position in the standing posture.

Fig. 7 shows the EER per propulsion angle. The propulsion energy was divided by the propulsion angle in each position and normalized according to the maximum energy among all positions. For the shorter subject group in the sitting posture, the EER per propulsion angle was the lowest in the DF position. EER was higher in the upward and backward directions and lower in the downward and forward directions. For the taller subject group, the EER per propulsion angle was the lowest in the UF position. EER was higher in the downward and backward directions and lower in the upward and forward directions. For the shorter subject group in the standing posture, the EER per propulsion angle was the lowest in the DC position and higher in the upward and backward positions. For the taller subject group, the EER per propulsion angle was the lowest in the MC position. The EER became higher when the position moved in any vertical or horizontal direction from the MC position.

3.5 Elbow flexion angle at the TDC

Fig. 8 shows the elbow flexion angle at the TDC in the sagittal plane. In the sitting posture, the elbow flexion angle of the shorter subjects was the smallest in the UC position (43.7° ± 12.1) and the largest in the DF position (70.3° ± 27.3). The downward positions had significantly higher elbow angles than the upward positions ($p < 0.05$). The elbow flexion angle of the taller subjects was the smallest in the UC position (50.4° ± 15.7) and the largest in the DF position (75.8° ± 15.7) (Fig. 8(a)). The downward positions had significantly higher elbow angles than the middle or upward positions ($p < 0.05$). In the standing posture, the elbow flexion angle of the shorter subjects was the smallest in the UB position (64.3° ± 11.3) and the largest in the DF position (77.5° ± 25.5). The elbow flexion angle of the taller subjects was the smallest in the UC position (57.8° ± 15.8) and the largest in the DC position (76.7° ± 15.6) (Fig. 8(b)). The downward positions had significantly higher elbow angles than the upward positions for both groups ($p < 0.05$).

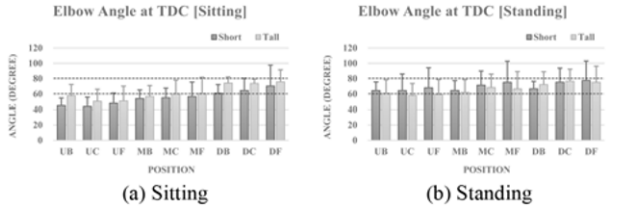

Fig. 8 Mean values of the elbow flexion angle at the top dead center (TDC) at each position

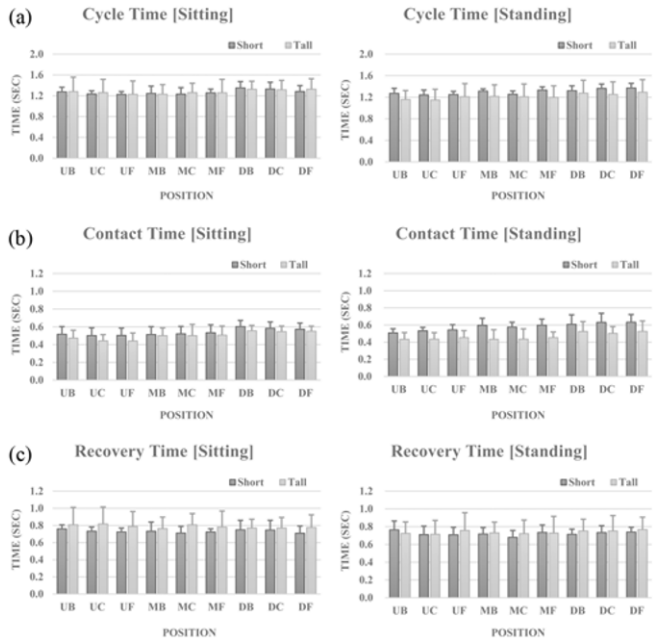

Fig. 9 Mean values of the propulsion cycle time at each position

3.6 Propulsion cycle time

Fig. 9 shows the propulsion cycle time at each position. The cycle time consists of contact time and recovery time. The mean cycle times were 1.27 ± 0.04 s and 1.26 ± 0.06 s in the sitting and standing postures, respectively (Fig. 9(a)). The mean contact times and recovery times were 0.52 ± 0.04 s and 0.76 ± 0.03 s in the sitting posture and 0.52 ± 0.07 s and 0.73 ± 0.02 s in the standing posture, respectively. The shorter subject group had a longer contact time than the taller subject group in all positions, and the downward position had a longer contact time than the middle or upward position (Fig. 9(b)). The taller subject group had a longer recovery time than the shorter subject group in the sitting posture; however, in the standing posture, there were no differences between the shorter and taller subject groups (Fig. 9(c)). The downward positions had significantly longer contact times than the upward positions in both postures ($p < 0.05$).

4. Discussion and Conclusions

4.1 Sitting – Shorter subject group

Changes in the energy expenditure were sensitive to the vertical and horizontal seat position changes. Energy expenditure increased when

the seat height was decreased. The horizontal seat movement did not affect the energy expenditure in the upward position. The difference between the highest and the lowest energy expenditures was about 30%. Shorter elderly individuals should be sitting in a forward position because their arms are not long enough to propel the hand rims. The positions with the lowest energy expenditure were the MF and the DF positions.

The propulsion angle was over 140° in the MC, MF, DB, DC, and DF positions, and the DF position had the largest angle of 166.9°. The EER per propulsion angle was 60.3%, which was the lowest EER in the DF position. The elbow angle at the TDC in the DF position was 70.3°, which met the preset criteria of 60° to 80°. Thus, the optimal propulsion position for the shorter elderly group was the DF position in the sitting posture.

4.2 Sitting – Taller subject group

Changes in the energy expenditure were sensitive to the vertical position changes. Especially in the backward seat positions, the energy expenditure increased rapidly with a decreasing seat height. When the subjects sat in the upward position, their energy expenditure did not significantly change. The difference between the highest and the lowest energy expenditures was about 30%. Taller elderly individuals should sit in a backward position because their arms are too long to propel the hand rims. The position with the lowest energy expenditure was the UB position, and the upward positions had smaller energy expenditures than the middle and/or downward positions.

The propulsion angle was over 140° in the MF, DC, and DF positions, and the MF position had the largest angle of 148.4°. The EER per propulsion angle was 60.4%, which was the lowest EER in the UF position, and the forward position had lower EERs than the other horizontal positions. The elbow angle at the TDC of the UF position was 50.9°, which did not meet the preset criteria of 60° to 80°. The MF position had the second lowest EER, with a propulsion angle of 148.4° and elbow angle of 60.8° at the TDC. Therefore, the MF position was a better optimal position for the taller elderly group in the sitting posture.

4.3 Standing – Shorter subject group

The position with the lowest energy expenditure was the MC position. The highest energy expenditure was shown in the DB position.

Except for the UB and UC positions, the propulsion angle was over 140° in all positions, and the DF position had the largest angle of 159.0°. The EER per propulsion angle was 83.1% in the DC and 84.4% in the MC position. All positions had a satisfying elbow angle between 60° to 80° at the TDC. Hence, the optimal propulsion position for the shorter elderly group in the standing posture was either the MC or DC position.

4.4 Standing – Taller subject group

The position with the lowest energy expenditure was the UC position. Energy expenditure was larger in the forward positions. The taller subjects have longer arms than the shorter subjects; thus, their optimal position was farther from the hand rims. The UC position had the lowest energy expenditure, and the center positions had lower energy expenditures than the backward or forward positions.

Except for the UB, UC, and MB positions, the propulsion angle was over 140° in all positions, and the MF position had the largest angle of 159.5°. The EER per propulsion angle was 87.7% in the MC position; however, the UC position had a 93.0% EER because it had the smallest propulsion angle. Except for the UC and UF positions, all positions had an elbow angle between 60° to 80° at the TDC. Although the UC position had the lowest propulsion energy, its propulsion angle and elbow angle did not fall in the recommended range. Therefore, the MC position was a more suitable optimal position for the taller elderly group in the standing posture.

4.5 Comparison with previous literature

In previous studies of wheelchair biomechanics, the upper extremity joint angle is very important with regards to the risk of injury and propulsion efficiency. As mentioned earlier, Van der Woude et al.[4] concluded that seat height adjustment is critical and related to anthropometric dimensions and that the optimum seat height is defined when the elbow angle is between 60-80° while the user grips the TDC of the hand rim. In this study, the elbow angles were different depending on the subjects' height and posture. The shorter subject group had a lower elbow angle than the taller subject group in the sitting posture, while the shorter subject group had a higher elbow angle than the taller subject group in the standing posture. However, both groups had a higher elbow angle in the downward positions than in the upward positions.

Masse et al.[5] investigated propulsion patterns and EMG for five male paraplegic patients in six seat positions. They concluded that the backward-low position had the overall lowest IEMG and demonstrated a smoother motion of the elbow and forearm. Kotajarvi et al.[6] showed that the tangential force output did not change with the seat position, and the axial and radial forces were largest in the lowest seat position because of an increased shoulder abduction. Therefore, they concluded that the propulsion efficiency did not significantly change with seat positions. However, they found that low seat positions improved the temporal variables, including contact time, recovery time, and push angle. It means that low seat positions may reduce strain on the upper limb and improve efficiency rather than high seat positions. Our study also showed similar results in that the contact time and the propulsion angle increased in the downward positions. Moreover, since the standing wheelchair in our study has separated hand rims, which are in front of the subject unlike a typical wheelchair, the seat height did not much affect the shoulder abduction.

In previous literature, a lower and backward seat position is more efficient than other seat positions in wheelchair propulsion. In a typical wheelchair, the center axle of the hand rim is located posterior to the subject's shoulder in the horizontal plane, and the TDC of the hand rim is about 10 to 12 cm higher than the seat. However, for the manual standing wheelchair in this study, the center axle of the hand rim was placed 35.3 cm anterior to the backrest and about 3.2 cm higher than the seat in the sitting posture. Therefore, the results of the propulsion biomechanics were different from those of prior studies. Most of the previous studies have investigated the seat positions of a typical wheelchair; therefore, it is difficult to compare the standing wheelchair with a typical wheelchair directly. However, we found that the subject's height in this study is a very important factor to determine the optimal seat position for the manual standing wheelchair with hand rims separated from the wheels.

In this study, the energy expenditures were obtained in multiple seat

and footrest positions for both the sitting and standing postures using a manual standing wheelchair and brake-type dynamometer. Further, the propulsion angle and the elbow angle were measured using a 3D motion capture system simultaneously. Ultimately, the subject's height was a very important factor in determining the optimal position. A manual standing wheelchair that can move in a standing posture could be very useful for patients in terms of physical mobility and psychological benefit, especially if it is adjusted to the optimal position for each user to prevent upper extremity injuries.

4.6 Limitations of the study

The measured data of this study were obtained using a wheelchair dynamometer; therefore, the results could be different with a level surface. However, Koontz et al.[15] reported that there was a high positive correlation between the biomechanical parameters measured from a level surface and a dynamometer, such as resultant force, tangential force, radial force, wheel-axle moment, and contact angle. Therefore, they concluded that both conditions have similar propulsion mechanisms.

Another limitation is that the axial force was not calculated in this study. Kortajarvi et al.[6] reported that the axial forces increased in too low seat positions because of an increased shoulder abduction. However, the hand rims of the standing wheelchair were located relatively higher than those of a typical wheelchair and had enough distance to the subjects. Therefore, it is supposed that the change in the axial force by shoulder abduction did not affect the determination of the optimal position.

However, owing to the differences in the diameter and location of the hand rims between the standing wheelchair and the typical wheelchair, it is assumed that an activation pattern of each upper extremity muscle would be changed. Further studies should investigate the contribution of each upper extremity muscle during the propulsion of the standing wheelchair.

ACKNOWLEDGEMENT

This research was supported by The Leading Human Resource Training Program of Regional Neo Industry through the National Research Foundation of Korea (NRF) funded by the Ministry of Science, ICT and Future Planning (No. 2016H1D5A1909760).

REFERENCES

1. Cooper, R. A., Boninger, M. L., and Robertson, R. N., "Heavy Handed: Repetitive Strain Injury among Manual Wheelchair Users," Team Rehab Report, Vol. 9, No. 2, pp. 35-38, 1998.
2. Subbarao, J. V., Klopfstein, J., and Turpin, R., "Prevalence and Impact of Wrist and Shoulder Pain in Patients with Spinal Cord Injury," The journal of Spinal Cord Medicine, Vol. 18, No. 1, pp. 9-13, 1995.
3. Brubaker, C., "Wheelchair Prescription: An Analysis of Factors that Affect Mobility and Performance," Journal of Rehabilitation Research and Development, Vol. 23, No. 4, pp. 19-26, 1986.
4. Van der Woude, L., Veeger, D.-J., Rozendal, R., and Sargeant, T., "Seat height in Handrim Wheelchair Propulsion," Journal of Rehabilitation Research and Development, Vol. 26, No. 4, pp. 31-50, 1989.
5. Masse, L. C., Lamontagne, M., and O'riain, M. D., "Biomechanical Analysis of Wheelchair Propulsion for Various Seating Positions," Journal of Rehabilitation Research and Development, Vol. 29, No. 3, pp. 12-28, 1991.
6. Kotajarvi, B. R., Sabick, M. B., An, K.-N., and Zhao, K. D., "The Effect of Seat Position on Wheelchair Propulsion Biomechanics," Journal of Rehabilitation Research and Development, Vol. 41, No. 3B, pp. 403-414, 2004.
7. Arva, J., Paleg, G., Lange, M., Lieberman, J., Schmeler, M., et al., "Resna Position on the Application of Wheelchair Standing Devices," Assistive Technology, Vol. 21, No. 3, pp. 161-168, 2009.
8. Karmarkar, A. M., Dicianno, B. E., Graham, J. E., Cooper, R., Kelleher, A., and Cooper, R. A., "Factors Associated with Provision of Wheelchairs in Older Adults," Assistive Technology, Vol. 24, No. 3, pp. 155-167, 2012.
9. Requejo, P. S., Furumasu, J., and Mulroy, S. J., "Evidence-Based Strategies for Preserving Mobility for Elderly and Aging Manual Wheelchair Users," Topics in Geriatric Rehabilitation, Vol. 31, No. 1, pp. 26-41, 2015.
10. Lin, C.-J., Lin, P.-C., Guo, L.-Y., and Su, F.-C., "Prediction of Applied Forces in Handrim Wheelchair Propulsion," Journal of Biomechanics, Vol. 44, No. 3, pp. 455-460, 2011.
11. Hwang, S., Kim, S., Son, J., Lee, J., and Kim, Y., "Upper Limb Joint Motion of Two Different User Groups during Manual Wheelchair Propulsion," Journal of the Korean Physical Society, Vol. 62, No. 4, pp. 648-656, 2013.
12. Kim, Y., Ryu, J., Son, J., Kim, S., and Hwang, S., "Wheelchair Propulsion Torque and Joint Moments during Manual Wheelchair Propulsion on a Brake-Type Dynamometer," Proc. of 15th International Conference on Biomedical Engineering, 2013.
13. Ryu, J., Son, J., Hwang, S., and Kim, Y., "Biomechanics in Manual Wheelchair Propulsion on a Brake-Type Dynamometer," Proc. of 7th World Congress of Biomechanics, 2014.
14. Ryu, J., Kim, S., Son, J., and Kim, Y., "Dynamometer Design for Biomechanical Analysis of Upper Extremity during Manual Wheelchair Propulsion," Proc. of the KSPE Spring Conference, pp. 1461-1462, 2013.
15. Koontz, A. M., Worobey, L. A., Rice, I. M., Collinger, J. L., and Boninger, M. L., "Comparison between Overground and Dynamometer Manual Wheelchair Propulsion," Journal of Applied Biomechanics, Vol. 28, No. 4, pp. 412-419, 2012.